

# Journal of Materials Chemistry A

Accepted Manuscript



This is an *Accepted Manuscript*, which has been through the Royal Society of Chemistry peer review process and has been accepted for publication.

*Accepted Manuscripts* are published online shortly after acceptance, before technical editing, formatting and proof reading. Using this free service, authors can make their results available to the community, in citable form, before we publish the edited article. We will replace this *Accepted Manuscript* with the edited and formatted *Advance Article* as soon as it is available.

You can find more information about *Accepted Manuscripts* in the [Information for Authors](#).

Please note that technical editing may introduce minor changes to the text and/or graphics, which may alter content. The journal's standard [Terms & Conditions](#) and the [Ethical guidelines](#) still apply. In no event shall the Royal Society of Chemistry be held responsible for any errors or omissions in this *Accepted Manuscript* or any consequences arising from the use of any information it contains.



## ARTICLE

## Amino Acid Mediated Mesopore Formation in LTA Zeolite†

Zhuwen Chen,<sup>a</sup> Jian Zhang,<sup>a</sup> Bole Yu,<sup>a</sup> Guangchao Zheng,<sup>a</sup> Jing Zhao,<sup>a,b</sup> and Mei Hong<sup>a\*</sup>cReceived 00th January 20xx,  
Accepted 00th January 20xx

DOI: 10.1039/x0xx00000x

www.rsc.org/

Mesoporous LTA zeolites have been hydrothermally synthesized by using amino acid as the mesoporegen. Amino acids of carnitine, lysine, or their salt derivatives were able to generate disordered mesopores of 10–20 nm within single crystalline LTA zeolites. Unlike other mesopore generating templates such as surfactants or polymers, the amino acid templates could be easily removed by washing with water, eliminating the energy-intensive calcination step. A possible crystallization process involving three-dimensional assembly of amino acid templates *via* hydrogen bonding and electrostatic interaction was proposed as hydrogen-bonding was found to be crucial in the hierarchical structure generation, and that hydroxyl group shielded acetyl carnitine yielded no mesopores. The obtained hierarchically mesoporous LTA zeolites exhibited remarkably higher adsorption capacity (264 mg/g) for catalase enzyme, and retained greater enzyme activity (> 90%) than did conventional LTA.

## 1. Introduction

Recent decade sees significant progress in the development of mesoporous zeolitic materials that possess hierarchical pore architectures.<sup>1–5</sup> The creation of mesopores into zeolite materials is highly desirable to overcome the great diffusion limitations imposed by the inherent micropores in the size range of 0.3–1.5 nm.<sup>6</sup> Various methods have been developed for creating mesoporosity in zeolites, including removal of framework atoms,<sup>7</sup> hard templating,<sup>8</sup> and soft templating.<sup>9,10</sup> Soft templates typically include surfactants or soft polymers which have relatively flexible structure. However, the ordinary surfactants, succeeded in the synthesis of amorphous mesoporous silica, resulted in phase separation when employed in the zeolite synthesis.<sup>11,12</sup> The supramolecular templating mechanism of the surfactant micelles that assisted the assembly of amorphous mesoporous materials acted competitively rather than cooperatively with the molecular templating mechanism for zeolites, leading to surfactant exclusion from the aluminosilicate domain during the zeolite crystallization process. To overcome this phase-segregation problem, specially designed or exquisitely chosen soft templates, including amphiphilic organosilanes,<sup>13–18</sup> bifunctional polyquaternary ammonium surfactants,<sup>9,10,19</sup> and cationic polymers,<sup>13,20,21</sup> have been successfully developed. The surfactants of dual functional

polyquaternary ammonium usually yielded lamellar or hexagonal zeolite structure on the mesoscale, while the organosilane surfactants yielded aggregated nanocrystals. Zhu et al.<sup>22</sup> ascribed this lack of long-range order phenomena to the thermodynamic and kinetic incompatibility of the zeolite framework generation process and the mesopore formation pathway, and even the specially designed surfactants still favored ordered mesostructures due to micelle formation, sacrificing the continuity of the zeolite framework. Therefore, they rationally chose cationic polymer templates with weaker interactions than surfactants to synthesize single crystalline zeolite with disordered mesopores, which exhibited excellent hydrothermal stability. Although purified cationic polymers mediated mesopore formation in zeolite beta, the small molecules such as monomers or structure units of polymers were not able to direct the structure of zeolite beta. Later on, Zhang et al.<sup>23</sup> reported that cationic center separation of the cationic polymer structure was important for the hierarchical structure generation in zeolites. While a copolymer of epichlorohydrin-*N,N*-dimethyl-1,3-diaminopropane copolymer (PCA) templated mesoporous ZSM-5 zeolite, its structural analogue of epichlorohydrin-dimethylamine polyamine (PCS) only led to bulky ZSM-5 zeolite crystals with low mesoporosity, because PCS completely decomposed in the hydrothermal synthesis conditions while the PCA stability improved due to the more widely separated cationic centers. On the basis of these previous observations, we hypothesize that by using small molecules having zwitterionic structures with positive and negative charge center widely separated, mesoporous zeolites might be achievable. The ionic small molecules would be advantageous over polymers due to their structure flexibility, high stability, and high solubility.

Inspired by the long-established biomineralization process,<sup>24, 25</sup> as well as the conformation-specific interaction between zeolite framework and biologically important molecules such as

<sup>a</sup> Guangdong Provincial Key Laboratory of Nano-Micro Materials Research, School of Chemical Biology & Biotechnology, Peking University Shenzhen Graduate School, Shenzhen 518055, China. E-mail: hongmei@pkusz.edu.cn

<sup>b</sup> Institute of Chemistry and BioMedical Sciences, State Key Laboratory of Pharmaceutical Biotechnology, School of Life Sciences, Nanjing University, Nanjing, 210093, China.

† Electronic supplementary information (ESI) available: Fig. S1–S7 are included. See DOI: 10.1039/x0xx00000x

amino acids,<sup>26-28</sup> we were attracted to the question whether these small molecules, while altering the zeolite crystallization kinetics,<sup>29-31</sup> could mediate mesopore formation. We embarked our study on LTA zeolite, the most hydrophilic zeolite with eight-membered ring apertures of 0.42 nm, having a Si/Al ratio of 1. Although extensive studies have been reported on the synthesis of mesoporous zeolites, reports on mesoporous LTA zeolite are rare. This partly lies in the fact that hard templates like carbon nanoparticles are incompatible with the hydrothermal synthesis condition of zeolite LTA framework, and it is not easy to synthesize mesoporous LTA zeolite even when carbon aerogel was used.<sup>32, 33</sup> The soft template like polymer may induce reversed crystal growth to form a core-shell structure with amorphous interior.<sup>33-37</sup> Ingeniously designed organosilane surfactants synthesized by multi-steps were first reported by Ryoo<sup>14</sup> and co-workers as mesopore generating templates in order to overcome the phase separation of surfactant micelles and the growing zeolite phase by covalently bonding to aluminosilicate structure. Then this method was continued by Ryoo and followed by other groups to synthesize mesoporous LTA zeolite.<sup>17,38-44</sup> It should be noted that the mesopore size was mostly smaller than 10 nm unless a pore expansion agent such as triblock copolymer Pluronic P123 was used simultaneously.<sup>17</sup> The mesopore templates used in these researches tend to be expensive and were encapsulated within or covalently bonded to the growing zeolite, which need a post-synthetic calcination step to release the mesoporosity.

In this study, we demonstrate for the first time that amino acid can work as an inexpensive mesopore generating agent to synthesize hierarchically structured LTA zeolite single crystals with mesopores larger than 10 nm in a one-pot hydrothermal synthesis. As a proof-of-concept study, we chose a standard amino acid L-lysine (Lys) and nonstandard amino acid L-carnitine (LC) having a permanent zwitterion form, as well as their salt derivatives L-lysine acetate (LysAc) and L-carnitine L-tartrate (LCLT). The structural flexibility of amino acids allowed their better incorporation into the zeolite crystals, and their stability and solubility ensured easy removal after the hydrothermal synthesis by a simple washing step, totally eliminating the need for the energy-intensive calcination process. With this novel approach, we successfully synthesized highly mesoporous LTA zeolites (named as MLTA-X-Y, where X is the utilized amino acid and Y is the synthesis stage.). The mesopore diameter peaked in the range of 15-20 nm, larger than the <10 nm mesopore diameter obtained from the surfactant-based strategies for mesoporous LTA zeolites,<sup>14,17,45-47</sup> making them highly suitable for large biomolecule adsorption and thus, the loading for catalase enzyme (CAT) were more than doubled for the current MLTA compared to conventional microporous LTA zeolite (CLTA). The low cost and high structure diversity of amino acids and their biocompatibility open door to easy access to a variety of hierarchical zeolites for industrially important applications as adsorbents, ion exchangers, and catalysts.

## 2. Experimental

### 2.1 Materials

All reagents were of analytical grade and used as purchased without further purification. Sodium hydroxide and catalase were purchased from Sigma-Aldrich, sodium aluminate from General-Reagent, and Ludox (25% aqueous solution) from Qingdao Ocean Co., Ltd. L-carnitine was obtained from Energy Chemical, tartaric acid from Beijing Ouhe Technology, calcium chloride from J&K, L-lysine, L-lysine acetate salt and O-acetyl-L-carnitine (AcLC) hydrochloride from Adamas-beta. Commercial LTA and FAU were purchased from Acros. Catalase assay kit was obtained from Beijing Solarbio Science & Technology Co., Ltd.

### 2.2 Synthesis of Mesoporous LTA Zeolites

Mesoporous LTA zeolites were synthesized using amino acids as the mesopore generating agents. In an example synthesis for MLTA-LC, 12.54 ml Ludox (25%) were dissolved in 20 ml deionized water, followed by a peristaltic pump addition of a clear solution containing 2.4 g NaOH and 4.92 g NaAlO<sub>2</sub> dissolved in 34 ml deionized water. After stirring at room temperature for 3 h, the solution was heated to 80 °C, and then a solution containing 4.8 g L-carnitine in 5 ml deionized water was dosed in. The resulting gel underwent crystallization at 100 °C for 20 h under constant stirring. The pH of the synthesis solution was monitored with pH electrode (Mettler Toledo FE20), which showed an alkaline reaction condition having pH between 13-14. The obtained powder was collected by a refrigerated centrifuge, and dried at 60 °C for more than 12 h, named as MLTA-LC-unwashed. The supernatant was also collected for characterization. Some MLTA-LC-unwashed samples were washed with deionized water until pH of the supernatant solution was close to 7, and dried at 60 °C for more than 12 h, designated as MLTA-LC-washed. To investigate the effect of high temperature calcination, some MLTA-LC-washed samples were calcined at 600 °C for 2 h in a muffle furnace, which were named as MLTA-LC-calcined.

The molar composition for MLTA-LC/ Lys and LTA-AcLC was 1Al<sub>2</sub>O<sub>3</sub>: 2SiO<sub>2</sub>: 2Na<sub>2</sub>O: 130H<sub>2</sub>O: 1 LC/ Lys/ AcLC respectively. For MLTA-LysAc, the composition was 1Al<sub>2</sub>O<sub>3</sub>: 2SiO<sub>2</sub>: 2Na<sub>2</sub>O: 130H<sub>2</sub>O: 0.5 LysAc, and for MLTA-LCLT, the composition was 1Al<sub>2</sub>O<sub>3</sub>: 2SiO<sub>2</sub>: 2Na<sub>2</sub>O: 130H<sub>2</sub>O: 0.25 LCLT.

Conventional LTA was synthesized in a procedure similar to MLTA except that no amino acid was added and the crystallization was conducted at 100 °C for 3 h. Commercial LTA with particle sizes of 1.8-2.3 μm was purchased from Acros as a reference sample.

### 2.3 Calcium Cation Exchange Experiment

The calcined MLTA materials were first cooled to room temperature, and then ion-exchanged with calcium cation by mixing 500 mg zeolites with a 5 ml solution of calcium chloride in a sealed tube at 80 °C for 6 h. The Ca<sup>2+</sup> exchanged zeolite was centrifuged, and washed by deionized water. This procedure was repeated twice, and then the collected sample was dried at 60 °C for more than 12 h. These samples were named as MLTA-X-Ca<sup>2+</sup>, where X is the utilized amino acid.

### 2.4 Catalase Adsorption Experiment

Fresh solutions of catalase were prepared by dissolving 50 mg catalase in 10 ml pH=7.2 phosphate buffer saline (PBS) solution at 0 °C under ultrasonic environment. 100 mg zeolite samples were added to the enzyme solution, and stirred at 4 °C by magnetic stirring at 600 rpm. 300  $\mu$ l suspension samples were periodically taken from the reaction mixture along the encapsulation process for characterization. Supernatants were collected via centrifugation at 10,000 rpm using a microcentrifuge and measured by a NanoDrop 2000c (Thermo Scientific) for the protein concentration measurements.

### 2.5 Catalase Activity Measurement

Fresh solutions of catalase were prepared by dissolving 20 mg catalase in 4 ml pH=7.2 phosphate buffer saline (PBS) solution at 0 °C under ultrasonic environment. 40 mg zeolite samples were added to the enzyme solution, and stirred at 4 °C by magnetic stirring at 600 rpm for 24h. Solid with immobilized catalase were collected via centrifugation at 10,000 rpm using a microcentrifuge, and dispersed in a PBS buffer to a catalase concentration of 0.05 mg/ml. Catalase activity was measured by using a catalase assay kit from Beijing Solarbio Science & Technology Co., Ltd (Product #BC0760). Catalase was incubated at 37 °C for 2 h before examination of the activities, and all assays were performed at 37 °C. Catalase activity unit (U) was defined as the amount of 1  $\mu$ mol hydrogen peroxide decomposed by 1 milligram catalase per second at 37 °C. The amount of degraded hydrogenperoxide was calculated by measuring the residual hydrogenperoxide concentration. The residual hydrogenperoxide was mixed with ammonium molybdate to form a complex with a maximum absorbance at wavelength of 405 nm.

### 2.6 Characterization

Powder X-ray diffraction (XRD) patterns of zeolite was recorded using a Rigaku D/Max-2200 PC diffractometer in the diffraction angle range  $2\theta = 4\text{--}50^\circ$  with Cu K $\alpha$  radiation ( $\lambda = 1.5418 \text{ \AA}$ ) at 40 KV, 40 mA. Scanning electron microscope (SEM) was performed on a JEOL JSM-7800F electron microscope operated at 5.0 KV without coating the samples. The transmission electron microscopy (TEM) was performed on a Tecnai G2 F30 field emission source transmission electron microscope operated at 300 kV. The zeolite samples were ultramicrotomed to a thickness of 90 nm for TEM measurement after being embedded in a spurr epoxy resin. Nitrogen adsorption-desorption isotherms were measured at -196 °C on a Micromeritics Tristar II 3020 v1.03 analyzer. The powder samples were degassed at 300 °C for at least 12 h before measurements. The Brunauer-Emmett-Teller (BET) surface areas were calculated from the adsorption data from  $0.05 < P/P_0 < 0.30$ . The mesopore size distributions were determined using the Barrett-Joyner-Halenda (BJH) model. The micropore volumes were determined using *t*-plot method. Si/Al ratios of as synthesized samples were measured by inductively coupled plasma-atomic emission spectroscopy (ICP-AES, JY 2000-2). Centrifugation of suspension samples were conducted by a refrigerated centrifuge (Thermo Scientific - Fiberlite F21s-8x50y). Thermogravimetric analyses (TGA) were performed on a Shimadzu TGA-50 analyzer.

Fourier Transform infrared spectroscopy FTIR spectra were recorded in KBr pellets on a Shimadzu IR-Prestige 21 Spectrophotometer.  $^1\text{H-NMR}$  and  $^{13}\text{C-NMR}$  measurements were performed on a 500 MHz nuclear magnetic resonance (NMR) (Bruker nuclear resonance spectrometer). For solid samples, 300 mg dry solid was dissolved in 10% hydrochloric acid solution or 5% hydrofluoric acid solution, followed by an evaporation and a drying step. The powders were dissolved into deuterioxide and filtered before a liquid NMR measurement. For liquid samples, 1 ml samples were dried and dehydrated, then dissolved into deuterioxide and filtered before a liquid NMR measurement. Protein concentrations were measured in a NanoDrop 2000c (Thermo Scientific). Absorbance value of hydrogenperoxide- molybdate complex was measured by a Shimadzu UV-2006 UV-Vis spectrophotometer.

## 3. Results and discussion

The powder X-ray patterns of the mesoporous LTA samples (Fig.1) all exhibited peaks that can be indexed onto the cubic unit cell of LTA zeolite framework structure. Referenced to commercial NaA zeolites, similar peak intensity with ca. crystallinity of 96%, 94%, 93% were obtained for CLTA, MLTA-LC-calcined, and MLTA-LCLT-calcined. The MLTA exhibited no obvious change of peak intensity and no distinct broadening of peak width, indicating the absence of nanocrystal aggregates, unlike surfactant mediated mesoporous LTA zeolite.<sup>14,17,48</sup> The structure of amino acid affected the crystal polymorph, while pure LTA was formed in the presence of LC, other amino acids slightly induced FAU phase of less than 10%. The content of FAU phase in the LTA zeolite was calculated using a homogeneous mixture of 10% commercial FAU/ 90 % commercial LTA purchased from Acros as a reference.

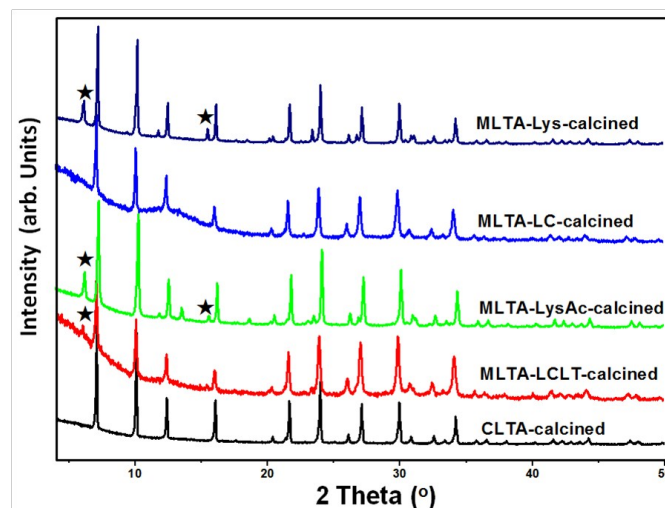


**Fig.1** Powder XRD patterns for mesoporous LTA synthesized with different amino acids and their derivatives: (a) Lys, (b) LC, (c) LysAc, (d) LCLT, in comparison with that for (e) conventional LTA counterpart. Diffraction peaks of FAU zeolite were marked with a ★. The powder samples were calcined at 600 °C for 2 h.

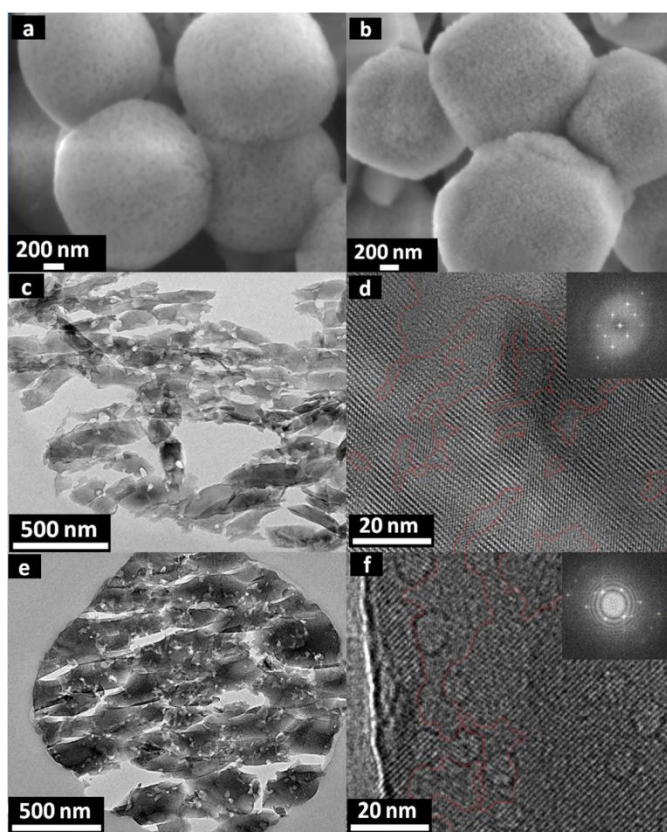


**Fig. 2** SEM (a,b) and TEM (c,d,e,f) images of washed mesoporous LTA synthesized with different amino acids and their derivatives: (a) MLTA-LC, (b) MLTA-LCLT, (c) Low-resolution TEM image and (d) HRTEM image of MLTA-LC, (e) Low-resolution TEM image and (f) HRTEM image of MLTA-LCLT, insets are the corresponding FFT diffractograms. Red marks were used in Fig. 2d and 2f as visual guide to the intracrystalline mesopore areas in LTA crystallites.

SEM images clearly revealed that all MLTA samples (Fig. 2a, 2b and Fig. S1a, 1b) preserved the cubic-shaped crystal outline with truncated edges typical of crystalline LTA with uniform particle sizes of about 1.1-1.4  $\mu\text{m}$ . The micro-sized cubic particles were polycrystalline in nature, as clearly demonstrated in low-resolution TEM images (Fig. 2c, 2e), showing that the cubic-shaped MLTA particles were composed of elongated large crystallites having size about  $100 \times 300$  nm. On the contrary, low resolution TEM image of conventional LTA samples (Fig. S1e) indicated that CLTA particles in the SEM images were single crystals. Different from the smooth surfaces of microporous LTA (Fig. S1c, 1d), MLTA samples exhibited obviously rugged surfaces indicating distribution of mesopores within the particles. Mesopores with average pore size about  $22.0 \pm 4.5$  nm for MLTA-LC and  $19.6 \pm 4.7$  nm for MLTA-LCLT were located within LTA crystallites. These mesopores were disordered as illustrated by the high-resolution TEM images (Fig. 2d, 2f), which also showed uniformly orientated lattice fringes over the entire

image regions confirming the single crystalline nature of the MLTA zeolites. Therefore, the mesopores created with the amino acid 'porogens' were confined within LTA crystallites, which in turn constituted cubic-shaped MLTA particles oriented in similar growth directions as CLTA. The crystal topology of MLTA samples, the clearly patterned fast Fourier transform (FFT, insets of Fig. 2d, 2f) diffractograms, and the high XRD peak intensity, all demonstrated high crystallinity with no amorphous components.

The micropore structure analyses of conventional NaA zeolites are well known to be unattainable from  $\text{N}_2$  adsorption isotherm measurement at 77 K because the micropore apertures in NaA zeolite are too narrow for  $\text{N}_2$  molecules to diffuse rapidly in a reasonable equilibrium time.<sup>17,49</sup> As expected, almost no  $\text{N}_2$  uptake was obtained for conventional LTA samples. The mesoporous MLTA samples, on the other hand, all showed a type IV  $\text{N}_2$  adsorption isotherms with a steep step at  $P/P_0$  in the range of 0.6-0.99 and a  $H_3$  hysteresis loop without any limiting adsorption at high  $P/P_0$  (Fig. 3a). This might be caused by capillary condensation of  $\text{N}_2$  gas in the mesopores,<sup>49,44</sup> leading to an increased BET surface area, as 90 and  $104 \text{ m}^2/\text{g}$  for MLTA-LC and MLTA-LCLT (Table 1). The mesopores (Fig. 3b) were between 10 to 50 nm, with distribution peak centered at 15-20 nm, consistent with those observed in TEM images. The pores generated by amino acids were much larger than the 6-10 nm mesopores mediated by amphiphilic organosilane surfactants.<sup>14</sup> For the organosilane templated mesoporous LTA, an additional pore expansion agent such as EO-PO-EO triblock copolymer was needed to further expand the mesopore size beyond 10 nm.<sup>17</sup>

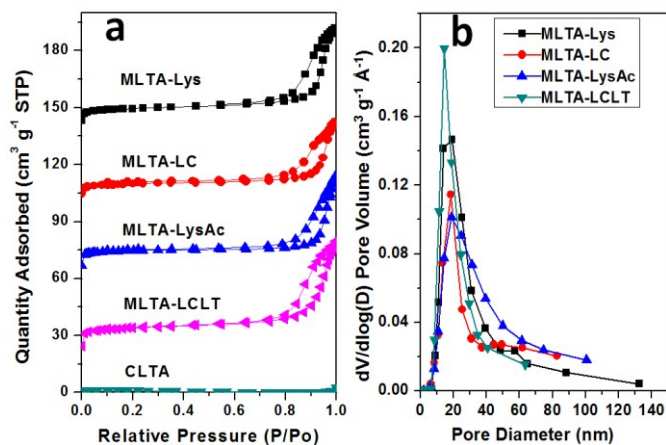


**Fig. 3** (a)  $\text{N}_2$  adsorption-desorption isotherms of washed mesoporous LTA synthesized with different amino acids and their derivatives in comparison with that for conventional LTA counterpart. The isotherms for MLTA-Lys, MLTA-LC, MLTA-LysAc were vertically offset by 120, 80, 40  $\text{cm}^3/\text{g}$  respectively. (b) BJH mesopore size distribution corresponding to the desorption branch. All samples were degassed at 300  $^\circ\text{C}$ .

Noting that only noncovalent interactions were expected between amino acids and zeolite framework, it is interesting to find out the

status of the amino acids in as-synthesized MLTA zeolites and whether water-washing could remove these organic mesopore generating agents. Characterization techniques including TGA, FTIR, and NMR were performed on the unwashed and washed MLTA samples, and compared to those on calcined samples, CLTA samples, and amino acid templates, which unambiguously proved the presence of amino acid in the as-synthesized MLTA samples and that water-washing could remove the amino acid template completely. The TGA profiles (Fig. 4) of MLTA-LC-unwashed showed a total weight loss of 29%, which was larger than the 19% for MLTA-LC-washed. The 10% weight loss difference could be attributed to the removal of residual L-carnitine template, which took place at a temperature range between 200-550 °C, similar to the temperature range for free L-carnitine decomposition. The

almost identical thermogravimetry profiles of MLTA-LC-washed, MLTA-LCLT-washed and CLTA samples with difference less than 5% (Fig. 4), also to that of calcined samples (Fig. S2), indicated similar nature and amount of adsorbed species on all LTA samples, despite the mesoporosity. The onset weight loss temperature at ~60 °C and inflection point at ~160 °C observed for washed MLTA samples, also identifiable in TGA curves for CLTA and the calcined MLTA samples, were probably associated with the dehydration of physically adsorbed water, and the progressive dehydration of entrapped water.<sup>44</sup> These TGA profiles were markedly different from those for free LC whose onset weight loss began at 237 °C (Fig. 4), demonstrating the lack of amino acid in the washed MLTA samples.

**Table 1.** Textural properties and catalase immobilization capacity of mesoporous LTA synthesized with various amino acids in comparison with those of conventional LTA samples.

Sample	$S_{\text{BET}}^{\text{a)}$ ( $\text{m}^2 \text{g}^{-1}$ )	$d_{\text{meso}}^{\text{b)}$ (nm)	$V_{\text{total}}^{\text{c)}$ ( $\text{cm}^3 \text{g}^{-1}$ )	$V_{\text{meso}}^{\text{d)}$ ( $\text{cm}^3 \text{g}^{-1}$ )	Si/Al <sup>e)</sup>	CAT ( $\text{mg g}^{-1}$ )	CAT activity <sup>f)</sup> ( $\text{U mg}^{-1}$ )	Relative activity <sup>g)</sup> (%)
CLTA	N.O. <sup>h)</sup>	N.O.	N.O.	N.O.	1.02	112	698.3	81.89
MLTA-LC	90	18.4	0.09	0.05	1.11	241	799.5	93.75
MLTA-LCLT	104	16.0	0.12	0.07	1.13	264	812.1	95.25
MLTA-Lys	89	19.1	0.11	0.07	1.16	179	815.7	95.66
MLTA-LysAc	141	19.0	0.12	0.07	1.14	208	768.7	90.15
CLTA- $\text{Ca}^{2+}$	476	<1.7	0.26	0.03	-	-	-	-
MLTA-LC- $\text{Ca}^{2+}$	492	18.3	0.30	0.07	-	-	-	-
MLTA-LCLT- $\text{Ca}^{2+}$	445	18.9	0.30	0.11	-	-	-	-
LTA-AcLC	1.5	N.O.	N.O.	N.O.	-	-	-	-

<sup>a)</sup> $S_{\text{BET}}$  is the BET surface area obtained from  $\text{N}_2$  adsorption isotherm in the relative pressure range of 0.05-0.30. <sup>b)</sup>Mesopore diameter calculated from the desorption branch using the BJH method. <sup>c)</sup>Total pore volume calculated as the amount of  $\text{N}_2$  adsorbed at  $P/P_0 = 0.98$ , <sup>d)</sup>Mesopore volume calculated as (total pore volume –  $V_{\text{mic}}$  obtained from t-Plot method). <sup>e)</sup>Si/Al ratio of as synthesized samples were measured by inductively coupled plasma-atomic emission spectroscopy (ICP – AES). <sup>f)</sup>CAT activity was calculated by  $\text{U mg}^{-1} = (\text{OD}_{\text{contrast}} - \text{OD}_{\text{sample}}) * 271 / 60 / m_{\text{CAT}}$ , CAT activity were measured after 24 hours. <sup>g)</sup>Relative activity was compared to the pure catalase with a CAT activity of  $852.7 \text{ U mg}^{-1}$ . <sup>h)</sup>N.O. data cannot be explicitly obtained. All samples were degassed at 300 °C for at least 12 h.

The FTIR spectra (Fig. 5) for MLTA-LC sample before and after water-washing and calcination, and CLTA sample all showed distinctive absorption bands at around 465, 559, 667 and 1003  $\text{cm}^{-1}$ , assigned to T–O (T = Si and Al) bending, external vibration of double rings ( $d4r$ ), internal vibration of T–O symmetric, and asymmetric stretching,<sup>50</sup> respectively of LTA structure. The intense band at 1640  $\text{cm}^{-1}$  can be ascribed to the bending mode in water molecule. Characteristic FTIR peaks of L-carnitine (Fig. 5) at 1582 and 1394  $\text{cm}^{-1}$ , assigned to carboxylate group, could be

found in the spectrum of MLTA-LC-unwashed sample, with a slight redshift to the wavenumbers of 1571 and 1379  $\text{cm}^{-1}$ .

Therefore, the amino acid of LC not only remained in the as-synthesized MLTA sample, but also interacted with the zeolite framework. These peaks were absent in the MLTA-LC-washed and MLTA-LC-calcined samples as well as the MLTA-LCLT-washed and MLTA-LCLT-calcined samples (Fig. S3), thus it is dubious that any amino acid was still present in the water-washed samples. <sup>13</sup>C-NMR spectrum of unwashed MLTA-LC samples (Fig. S4b) showed all the characteristic peaks of L-carnitine template,

similar to that of the filtered synthesis solution (Fig. S4a). For the water-washed MLTA-LC samples, neat  $^{13}\text{C}$ -NMR exhibited no residual organic molecules (Fig. S5b) and  $^1\text{H}$ -NMR (Fig. S5a) only showed a sharp peak of water. The complete disappearance of the L-carnitine peaks in the  $^{13}\text{C}$ -NMR spectra after the as synthesized MLTA was washed with water proved the effectiveness of water-washing. Therefore, we can be sure that amino acid templates could be totally removed by a simple step of water-washing, without the need for a calcination step. The almost identical SEM images and pore structure analysis results obtained for MLTA-LC-washed and MLTA-LC-calcined further supported this conclusion.

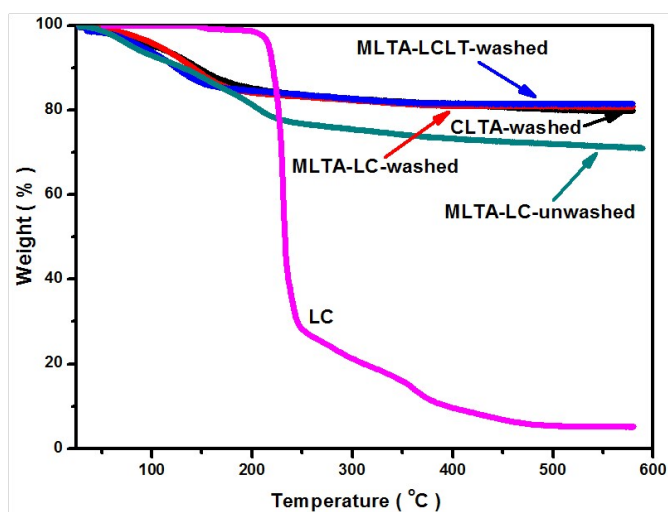


**Fig. 4** Relative weight loss by TGA of as synthesized MLTA-LC and MLTA-LCLT samples after water washing in comparison with that of as synthesized CLTA, MLTA-LC-unwashed and free carnitine. All samples were degassed at 110°C.

The mesopores were stable upon calcination and ion exchange. Both the crystal morphology (Fig. 6a, 6b) and the  $\text{N}_2$  adsorption-desorption isotherms (Fig. 6c), as well as the mesopore size distribution (Fig. 6d) were almost not altered. Calcium exchange increased the adsorbed amount of nitrogen and BET surface area (Table 1) as  $\text{Ca}^{2+}$  cation is known to increase the  $\alpha$ -cage aperture to 0.48 nm, enough for rapid uptake of  $\text{N}_2$  molecules with kinetic diameter of 0.44 nm into LTA zeolite framework micropores. The calcium exchange further confirmed the lack of mesopores in CLTA powders as the BJH pore size of CLTA- $\text{Ca}^{2+}$  was less than 1.7 nm.

The quaternary ammonium group in these amino acids probably acted as a structure-directing agent for hierarchical zeolites, similar to the cases for cationic polymer-based dual function templates, which strongly interacted with the negatively charged aluminosilicate framework *via* Coulomb forces. On the other hand, the 15–20 nm average mesopore diameters were too large to be explained by molecular size of the amino acids and their derivatives.

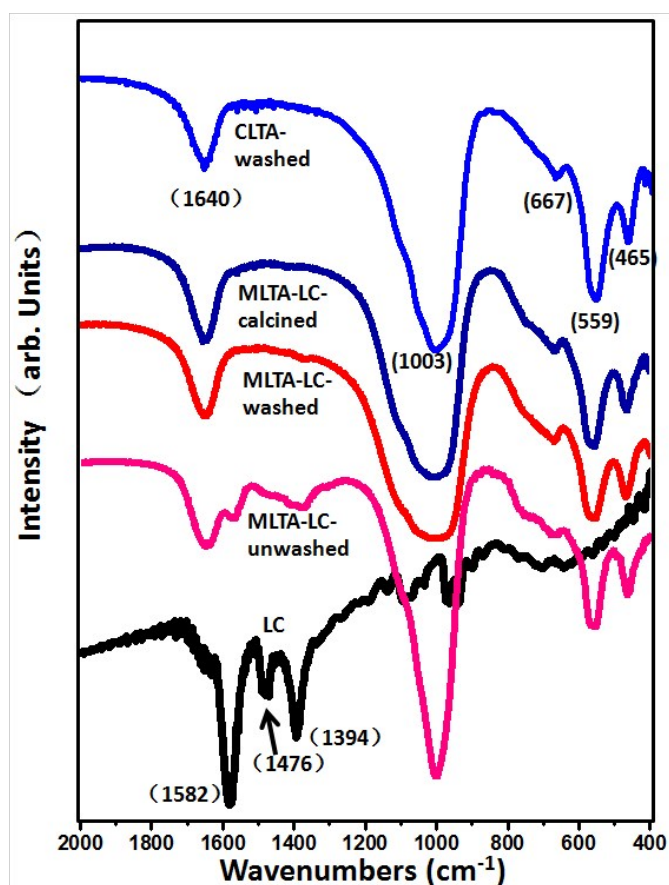


**Fig. 5** FTIR spectra of MLTA-LC sample as synthesized, after water-washing, and after calcination at 600°C, in comparison with that of as synthesized CLTA, and free carnitine. All samples were degassed at 110°C.

Self-assembly of amino acids within the confined space of growing MLTA *via* strong hydrogen bonding were suspected to be the main reason, and thus carnitine structure analogue of O-acetyl-L-carnitine with the side chain hydroxyl group protected was used to elucidate the mesopore formation mechanism.

Shielding the hydrogen bonds of carnitine resulted in smooth cubic LTA crystals (Fig. 7) with a BET surface area of only 1.5  $\text{m}^2/\text{g}$  (Table 1) and no mesopores. Therefore, hierarchical structure likely started from the cooperative assembly *via* electrostatic interactions between negatively charged framework of prezeolitic units and 3 dimensional network of amino acids linked by extensive hydrogen bonding (Scheme 1). The mesopore size range of 10–50 nm was in consensus with the prebiotic organic polymer system on mineral surfaces, having desired lengths in the range of 30–100 mers of amino acids.<sup>51</sup> Absence of covalent bonding with the zeolite framework and the high solubility of amino acids in water allowed their dissolution into the washing water.

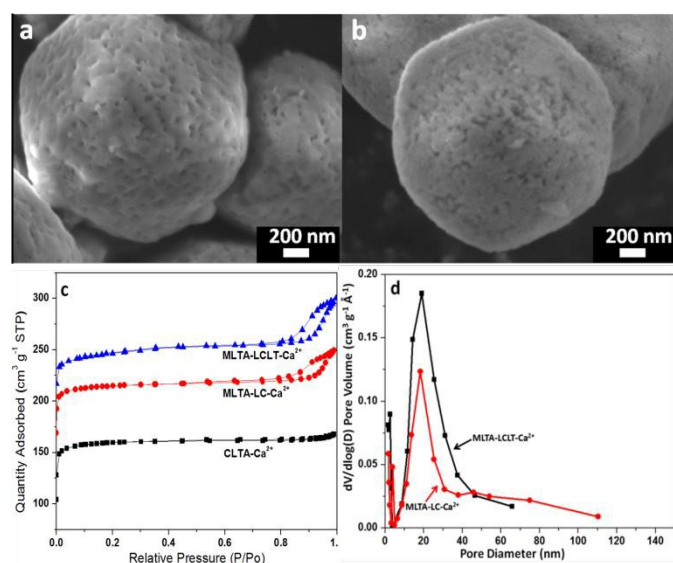
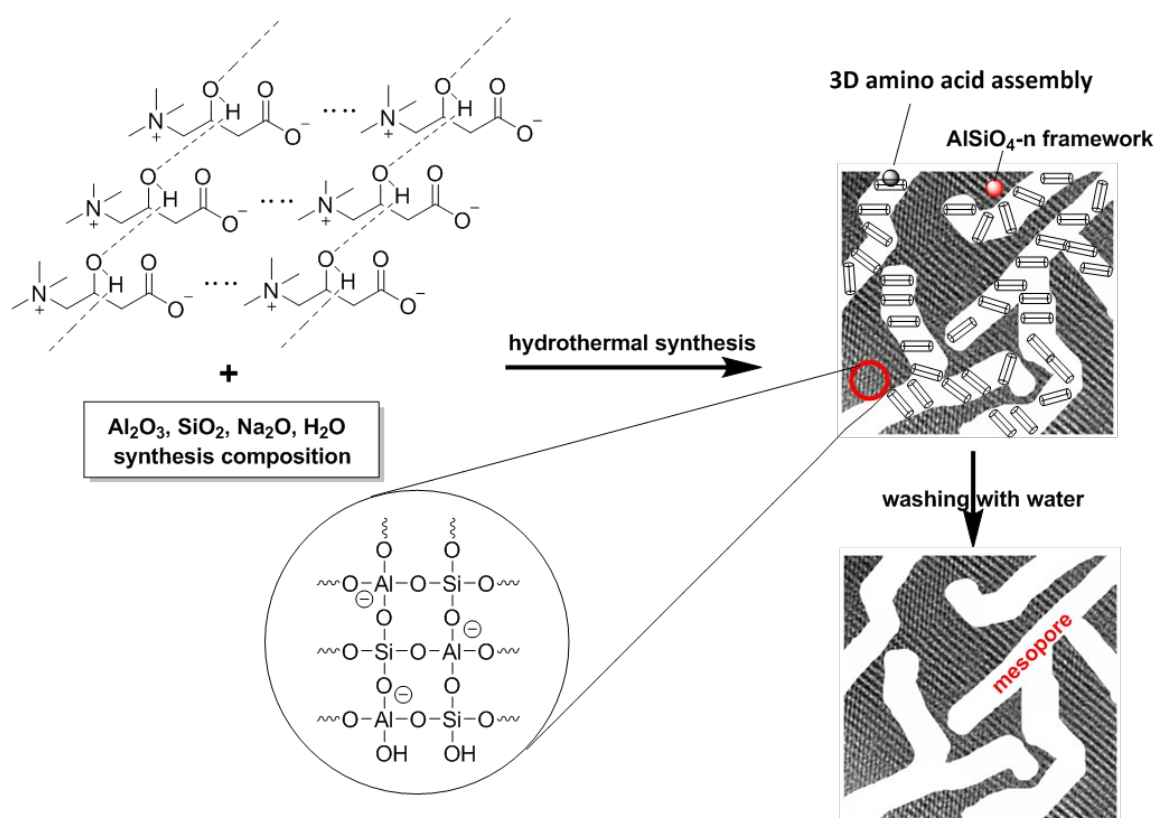


**Fig. 6** Properties of calcined and  $\text{Ca}^{2+}$  exchanged mesoporous LTA samples: (a) SEM images of MLTA-LC- $\text{Ca}^{2+}$ , (b) SEM images of MLTA-LCLT- $\text{Ca}^{2+}$  (c)  $\text{N}_2$  adsorption-desorption isotherms, the isotherms for MLTA-LC- $\text{Ca}^{2+}$  and MLTA-LCLT- $\text{Ca}^{2+}$  were vertically offset by 50 and 100  $\text{cm}^3 \text{g}^{-1}$ , respectively. (d) BJH mesopore size distribution corresponding to the desorption branch.

The creation in a biologically compatible way of hierarchical structures containing  $>10$  nm mesopores can be a remarkable benefit for immobilization and encapsulation of biomacromolecules, which could not enter the small micropores in conventional LTA. Therefore, immobilization of relatively large enzymes was tested. The bovine liver catalase enzyme (hydrogen peroxide oxidoreductase EC 1.11.1.6) is a glycoprotein containing four polypeptide chains, each over 500 amino acids long, with a molecular size of  $\sim 10$  nm, and is widely used in industry for catalyzing the degradation of hydrogen peroxide into water and oxygen. The mesoporous MLTA samples all exhibited a much higher catalase enzyme adsorption capacity (e.g., 264 mg/g for MLTA-LCLT), more than doubled than that of conventional LTA (Fig. 8). The adsorption kinetics were almost identical after the MLTA samples were calcined (Fig. S6), again confirming that the enhanced adsorption was due to the mesopores created by the amino acid 'porogen' that could be fully removed by a simple washing step. As zeolite LTA with low Si/Al ratio is famous for its extreme hydrophilicity, such a high enzyme immobilization capacity was probably due to electrostatic interaction and hydrogen bonding. The absence of hydrophobic effect could better protect the enzymes from denaturation induced by conformation change to expose their hydrophobic residues which are normally buried within the enzyme molecule.<sup>52</sup>



**Scheme 1.** Proposed mechanism for amino acid mediated mesoporous LTA formation



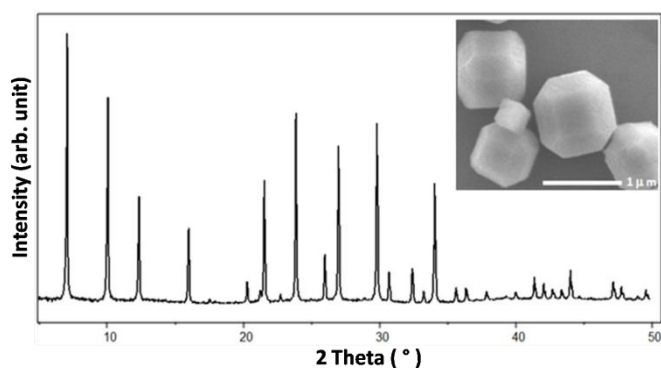


**Fig.7** Powder XRD pattern for LTA synthesized with O-Acetyl-L-carnitine hydrochloride, while the inset corresponds to the SEM image. The powder samples were calcined at 600 °C for 2 h.

As a result, the catalase enzyme immobilized on all MLTA samples retained more than 90% enzymatic activity of the equivalent free catalase molecules (Table 1), much higher than the <20% reported for functionalized carbon nanotubes,<sup>53</sup> ~5% for graphite,<sup>54</sup> or <3% for the metal-organic framework ZIF-90.<sup>52</sup> This suggests that the hydrophilic MLTA mesopore surfaces induced almost no structural change of catalase during adsorption process. The conventional LTA exhibited 82% retained catalase enzyme activity, ~10% lower than the hierarchical MLTA samples, probably due to the mass transport limitations or the non-optimized interface between LTA and catalase. To demonstrate the storage stability of the immobilized enzyme, all samples were stored at 4 °C in a refrigerator for 15 days. Almost no decline in catalase activity was detected, especially for MLTA-LCLT with the highest catalase loading (Fig. S7). The superiority of mesoporous LTA zeolites mediated by amino acids implies that this material can be used as a cheap and safe protein medicament carrier in the future.

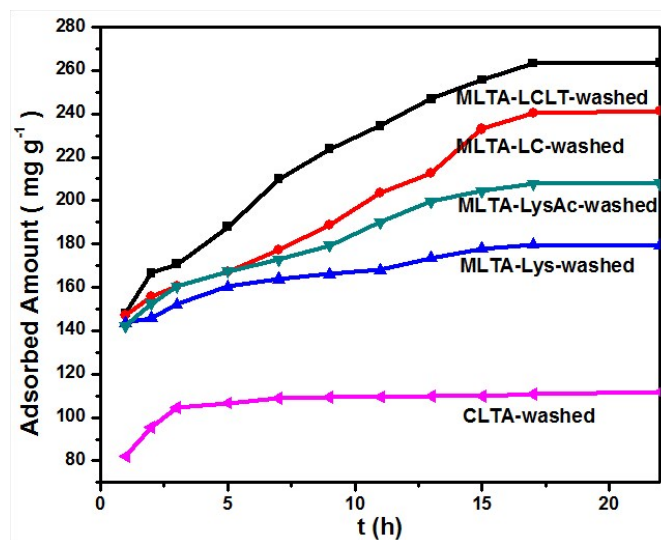


**Fig.8** Catalase adsorption kinetics on water-washed MLTA synthesized with different amino acids and CLTA. All samples were degassed at 110°C.

#### 4. Conclusions

In summary, we developed a new strategy for synthesizing mesoporous zeolite using amino acids as the mesopore-generating agents. A variety of amino acids have shown the ability to direct mesopore formation in zeolite LTA. This novel approach exhibited several advantages including easy handling, easy to scale up, and environmentally friendly. The mesoporous MLTA zeolite features large surface area, large mesopores over 10 nm, higher adsorption capacity towards large biomolecules, and higher retained activity of immobilized enzyme. The use of non-surfactant and non-polymeric biomolecule template ensured high crystallinity of the zeolite framework and easy template removal by simple washing, substituting the energy-consuming calcination process. We believe that this novel synthesis strategy can be employed to a wide range of zeolite structures, opening door to a new range of zeolitic materials. In addition to enzyme immobilization, the mesoporous zeolites produced in the present approach have great potential for other important applications such as heterogeneous catalysis, building segments for separation membranes, and drug delivery vehicles. Relevant studies on the synthesis mechanism as well as potential applications are currently underway.

## Acknowledgements

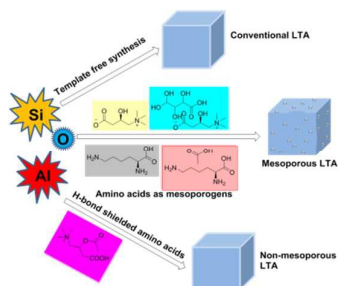
We thank Dr. Lianbing Ren and Dr. Chao Teng for helpful discussion. Financial support was provided by the Guangdong Government (2013A061401002), Shenzhen Government (SGLH20131010153302024, JCYJ20140419131807792, CXZZ20140419131807788), the Nanshan District of Shenzhen, China (FG2014JNYF0017A). Z.C would like to thank PKUSZ Dean' fund (2014013)

## Notes and references

- S. Lopez-Orozco, A. Inayat, A. Schwab, T. Selvam and W. Schwieger, *Adv. Mater.*, 2011, **23**, 2602.
- L.-H. Chen, X.-Y. Li, J. C. Rooke, Y.-H. Zhang, X.-Y. Yang, Y. Tang, F.-S. Xiao and B.-L. Su, *J. Mater. Chem.*, 2012, **22**, 17381.
- D. P. Serrano, J. M. Escola and P. Pizarro, *Chem. Soc. Rev.*, 2013, **42**, 4004.
- K. Moller and T. Bein, *Chem. Soc. Rev.*, 2013, **42**, 3689.
- Y. Wei, T. E. Parmentier, K. P. de Jong and J. Zecevic, *Chem. Soc. Rev.*, 2015, **44**, 7234.
- L. Gueudre, M. Milina, S. Mitchell and J. Perez-Ramirez, *Adv. Funct. Mater.*, 2014, **24**, 209.
- V. Valtchev, G. Majano, S. Mintova and J. Perez-Ramirez, *Chem. Soc. Rev.*, 2013, **42**, 263.
- R. J. White, A. Fischer, C. Goebel and A. Thomas, *J. Am. Chem. Soc.*, 2014, **136**, 2715.
- K. Na, C. Jo, J. Kim, K. Cho, J. Jung, Y. Seo, R. J. Messinger, B. F. Chmelka and R. Ryoo, *Science*, 2011, **333**, 328.
- D. D. Xu, Y. H. Ma, Z. F. Jing, L. Han, B. Singh, J. Feng, X. F. Shen, F. L. Cao, P. Oleynikov, H. Sun, O. Terasaki and S. N. Che, *Nat. Commun.*, 2014, **5**.
- L. M. Huang, W. P. Guo, P. Deng, Z. Y. Xue and Q. Z. Li, *J. Phys. Chem. B*, 2000, **104**, 2817.
- S. C. Christiansen, D. Y. Zhao, M. T. Janicke, C. C. Landry, G. D. Stucky and B. F. Chmelka, *J. Am. Chem. Soc.*, 2001, **123**, 4519.
- H. Wang and T. J. Pinnavaia, *Angew. Chem.-Int. Edit.*, 2006, **45**, 7603.
- M. Choi, H. S. Cho, R. Srivastava, C. Venkatesan, D. H. Choi and R. Ryoo, *Nat. Mat.*, 2006, **5**, 718.
- M. Choi, R. Srivastava and R. Ryoo, *Chem. Commun.*, 2006, 4380.
- R. Srivastava, M. Choi and R. Ryoo, *Chem. Commun.*, 2006, 4489.
- K. Cho, H. S. Cho, L. C. de Menorval and R. Ryoo, *Chem. Mat.*, 2009, **21**, 5664.
- A. Inayat, I. Knoke, E. Spiecker and W. Schwieger, *Angew. Chem.-Int. Edit.*, 2012, **51**, 1962.
- Y. Seo, S. Lee, C. Jo and R. Ryoo, *J. Am. Chem. Soc.*, 2013, **135**, 8806.
- F. S. Xiao, L. F. Wang, C. Y. Yin, K. F. Lin, Y. Di, J. X. Li, R. R. Xu, D. S. Su, R. Schlogl, T. Yokoi and T. Tatsumi, *Angew. Chem.-Int. Edit.*, 2006, **45**, 3090.
- D. H. Park, S. S. Kim, H. Wang, T. J. Pinnavaia, M. C. Papapetrou, A. A. Lappas and K. S. Triantafyllidis, *Angew. Chem.-Int. Edit.*, 2009, **48**, 7645.
- J. Zhu, Y. H. Zhu, L. K. Zhu, M. Rigutto, A. van der Made, C. G. Yang, S. X. Pan, L. Wang, L. F. Zhu, Y. Y. Jin, Q. Sun, Q. M. Wu, X. J. Meng, D. L. Zhang, Y. Han, J. X. Li, Y. Y. Chu, A. M. Zheng, S. L. Qiu, X. M. Zheng and F. S. Xiao, *J. Am. Chem. Soc.*, 2014, **136**, 2503.
- Y. Zhang, K. Zhu, X. Duan, X. Zhou and W. Yuan, *J. Mater. Chem. A*, 2014, **2**, 18666.
- H. Shiraga, W. Min, W. J. Vandusen, M. D. Clayman, D. Miner, C. H. Terrell, J. R. Sherbotie, J. W. Foreman, C. Przysiecki, E. G. Neilson and J. R. Hoyer, *Proc. Natl. Acad. Sci. U. S. A.*, 1992, **89**, 426.
- S. Albeck, J. Aizenberg, L. Addadi and S. Weiner, *J. Am. Chem. Soc.*, 1993, **115**, 11691.
- G. Yang and L. J. Zhou, *Sci. Rep.*, 2014, **4**.
- K. Stuckenschneider, J. Merz and G. Schembecker, *J. Phys. Chem. C*, 2014, **118**, 5810.
- M. Bouchoucha, F. Tielens, F. Gaslain, F. CostaTorro, S. Casale, A. Palcic, V. Valtchev, J. F. Lambert and M. Jaber, *J. Phys. Chem. C*, 2015, **119**, 8736.
- R. Watanabe, T. Yokoi and T. Tatsumi, *J. Colloid Interface Sci.*, 2011, **356**, 434.
- Y. Q. Deng, S. F. Yin and C. T. Au, *Ind. Eng. Chem. Res.*, 2012, **51**, 9492.
- J. Dhainaut, T. J. Daou, N. Bats, B. Harbuzaru, G. Lapisardi, L. Rouleau and J. Patarin, *Micropor. Mesopor. Mat.*, 2013, **170**, 346.
- Y. Tao, H. Kanoh and K. Kaneko, *Langmuir*, 2005, **21**, 504.
- H. Y. Chen, J. Wydra, X. Y. Zhang, P. S. Lee, Z. P. Wang, W. Fan and M. Tsapatsis, *J. Am. Chem. Soc.*, 2011, **133**, 12390.
- H. Greer, P. S. Wheatley, S. E. Ashbrook, R. E. Morris and W. Zhou, *J. Am. Chem. Soc.*, 2009, **131**, 17986.
- L. Han, J. Yao, D. Li, J. Ho, X. Zhang, C.-H. Kong, Z.-M. Zong, X.-Y. Wei and H. Wang, *J. Mater. Chem.*, 2008, **18**, 3337.
- S. Tanaka, N. Nakatani, H. Okada and Y. Miyake, *Top. Catal.*, 2010, **53**, 224.
- L. Bonaccorsi, P. Calandra, M. A. Kiselev, H. Amenitsch, E. Proverbio and D. Lombardo, *Langmuir*, 2013, **29**, 7079.
- M. Choi, D. H. Lee, K. Na, B. W. Yu and R. Ryoo, *Angew. Chem.-Int. Edit.*, 2009, **48**, 3673.
- D. H. Lee, M. Choi, B. W. Yu, R. Ryoo, A. Taher, S. Hossain and M. J. Jin, *Adv. Synth. Catal.*, 2009, **351**, 2912.
- R. Valiullin, J. Kärger, K. Cho, M. Choi and R. Ryoo, *Micropor. Mesopor. Mat.*, 2011, **142**, 236.
- K. Cho, R. Ryoo, S. Asahina, C. Xiao, M. Klingstedt, A. Umemura, M. W. Anderson and O. Terasaki, *Solid State Sci*, 2011, **13**, 750.
- F. Yan Chao, M. Ying, L. Fu Xiang, L. Zhi Ping and X. Jian Wei, *J. Porous Mat.*, 2013, **20**, 465.
- G. Q. Song, H. T. Liu, F. X. Li, Z. P. Lv and J. W. Xue, *J. Porous Mat.*, 2014, **21**, 1101.
- F. Hasan, R. Singh and P. A. Webley, *Micropor. Mesopor. Mat.*, 2012, **160**, 75.
- X. Zhaoteng, M. Jinghong, H. Wenming, B. Xiang, K. Yuhong, L. Jianhong and L. Ruifeng, *J. Mater. Chem.*, 2012, **22**, 2532.
- J. Kim, C. Jo, S. Lee and R. Ryoo, *J. Mater. Chem. A*, 2014, **2**, 11905.
- G. Rioland, S. Albrecht, L. Josien, L. Vidal and T. J. Daou, *New J. Chem.*, 2015, **39**, 2675.
- F. Hasan, R. Singh, G. Li, D. Zhao and P. A. Webley, *J. Colloid Interface Sci.*, 2012, **382**, 1.

49. K. S. W. Sing, D. H. Everett, R. A. W. Haul, L. Moscou, R. A. Pierotti, J. Rouquerol and T. Siemieniowska, *Pure Appl. Chem.*, 1985, **57**, 603.
50. E. HM.FLANIGEN, H. KHATAMI and H. A. SZYMANSKI, in *In Molecular Sieve Zeolites-I*, ed. E. Flanigen, et al., American Chemical Society: Washington, DC, 1974, vol. Advances in Chemistry.
51. I. Parsons, M. R. Lee and J. V. Smith, *Proc. Natl. Acad. Sci. U. S. A.*, 1998, **95**, 15173.
52. F. K. Shieh, S. C. Wang, C. I. Yen, C. C. Wu, S. Dutta, L. Y. Chou, J. V. Morabito, P. Hu, M. H. Hsu, K. C. W. Wu and C. K. Tsung, *J. Am. Chem. Soc.*, 2015, **137**, 4276.
53. C. Zhang, S. Luo and W. Chen, *Talanta*, 2013, **113**, 142.
54. R. C. Sosa, R. F. Parton, P. E. Neys, O. Lardinois, P. A. Jacobs and P. G. Rouxhet, *Journal of Molecular Catalysis A: Chemical*, 1996, **110**, 141.

# A table of contents



Amino acids, self-assembled *in situ* via hydrogen bonding, have been used to synthesize mesoporous zeolites without a calcination step.